Confocal scanning laser ophthalmoscopy improvement by use of Mueller-matrix polarimetry

Juan M. Bueno

Laboratorio de Óptica, Departamento de Física, Universidad de Murcia, Campus de Espinardo, Edificio C, 30071 Murcia, Spain, and School of Optometry, University of Waterloo, Waterloo, Ontario, Canada N2L 3G1

Melanie C. W. Campbell

School of Optometry, University of Waterloo, Waterloo, Ontario, Canada N2L 3G1

Received November 8, 2001

A new technique for improving the signal-to-noise ratio and the contrast in images recorded with a confocal scanning laser system is presented. The method is based on the incorporation of a polarimeter into the setup. After the spatially resolved Mueller matrix of a sample was calculated, images for incident light with different states of polarization were reconstructed, and both the best and the worst images were computed. In both the microscope and the opthalmoscope modes, the best images are better than the originals. In contrast, the worst images are poorer. This technique may be useful in different fields such as confocal microscopy and retinal imaging. © 2002 Optical Society of America

OCIS codes: 120.5410, 120.3890, 330.5370, 170.1790.

For more than four decades, confocal scanning laser microscopy has been used successfully to analyze samples in many diverse fields, ranging from biology[1] to the characterization of materials.[2] Webb *et al.*[3] presented the confocal scanning laser ophthalmoscope for viewing the ocular fundus by use of the ocular optics as a microscope objective. Since the optics of the eye degrade the image, additional improvements such as adaptive optics,[4] deconvolution techniques,[5] or changes in the beam diameter and its entry position in the pupil of the eye[6] have been made to fundus imaging.

The polarization properties of light have been used in conjunction with imaging techniques in target detection,[7] optical coherence tomography,[8,9] ophthalmologic diagnosis,[10] remote sensing,[11] and microscopy.[12] In general, optical imaging with polarization has been reported to improve contrast, reduce noise, and provide useful information about scenes (not available with polarization-blind imaging). Structural information (for example, nerve fiber layer thickness[10]) obtained from the polarization properties is also useful. In this Letter we propose the use of Mueller-matrix polarimetry to reduce noise and improve images recorded with a confocal scanning laser system.

A polarimeter[13] composed of a fixed linear polarizer, a rotating quarter-wave plate in the generator unit, and a symmetric configuration in the analyzer unit was incorporated into a confocal scanning laser microscope. Figure 1 shows a schematic diagram of the setup. The system was used in both microscope and ophthalmoscope modes. In the former, the focal length and the numerical aperture for the objective were 90 mm and 0.11, respectively; in the latter, the eye itself acted as a microscope objective. A 633-nm He–Ne laser was used as the light source and a photomultiplier tube as the detector. The laser beam was scanned in two dimensions and focused on the sample (a target or the retina) by the objective or the ocular optics. The light reflected back from the sample at each point of the scan was recorded by the detector. The size of the beam entering the objective (and the eye) was 2.5 mm, and the confocal pinhole was 600 μm in diameter. The focal length of the collector lens was 50 mm. The system records images at 28.5 Hz.

The 16 combinations of polarization states required for calculating the Mueller matrix for each point of the scanned sample correspond to different angles of the fast axes of the two rotating quarter-wave plates as previously described.[14]

For every Stokes vector $S_G^{(m)}$ ($m = 1, 2, 3, 4$) produced by the generator, the intensity reaching the detector for each point of the sample, $[I^{(mn)}]$, is the first element of Stokes vector $S_D^{(mn)}$ ($n = 1, 2, 3, 4$), given by

$$S_D^{(mn)} = \overline{M}_A^{(n)} M_{\mathrm{SCN}}^{(2)} M M_{\mathrm{SCN}}^{(1)} S_G^{(m)}, \tag{1}$$

where $M = M_{ij}$ ($i, j = 0, 1, 2, 3$) is the Mueller matrix of the sample under study, $\overline{M}_A^{(n)}$ is one of the four Mueller matrices of the analyzer unit (each

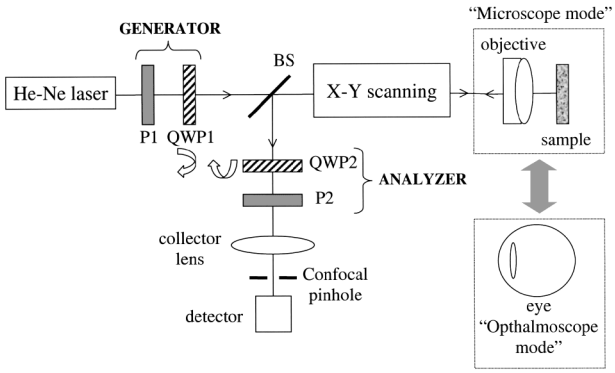

Fig. 1. Simplified schematic diagram of the experimental setup. P1, P2, linear horizontal polarizers; QWP1, QWP2, rotating quarter-wave plates. Both microscope and ophthalmoscope configurations are shown.

0146-9592/02/100830-03$15.00/0

corresponding to an independent state), and $M_{\mathrm{SCN}}^{(1)}$ and $M_{\mathrm{SCN}}^{(2)}$ are the Mueller matrices of the experimental system itself (lenses, scanning unit, and beam splitter) for the first and second passages, respectively, as previously measured in a calibration process. For each generator–analyzer combination, the image is spatially resolved, giving a spatially resolved value of M. Let M_A be the 4×4 auxiliary matrix, with each row being the first row of every $\overline{M}_A^{(n)}$, and $M_{\mathrm{OUT}} = [S_{\mathrm{OUT}}^{(1)}, S_{\mathrm{OUT}}^{(2)}, S_{\mathrm{OUT}}^{(3)}, S_{\mathrm{OUT}}^{(4)}]$ be another auxiliary matrix with $S_{\mathrm{OUT}}^{(m)}$ each Stokes vector going into the analyzer unit. These matrices are then related:

$$\begin{bmatrix} I^{(11)} & I^{(21)} & I^{(31)} & I^{(41)} \\ I^{(12)} & I^{(22)} & I^{(32)} & I^{(42)} \\ I^{(13)} & I^{(23)} & I^{(33)} & I^{(43)} \\ I^{(14)} & I^{(24)} & I^{(34)} & I^{(44)} \end{bmatrix} = M_A M_{\mathrm{OUT}}. \qquad (2)$$

If $M_G = [S_G^{(1)}, S_G^{(2)}, S_G^{(3)}, S_G^{(4)}]$, then M is computed by means of

$$M = \left[M_{\mathrm{SCN}}^{(2)}\right]^{-1} M_{\mathrm{OUT}} (M_G)^{-1} \left[M_{\mathrm{SCN}}^{(1)}\right]^{-1}, \qquad (3)$$

where M_{OUT} is obtained by inversion of Eq. (2).

From the spatially resolved Mueller matrix, images of the sample $I^{(\mathrm{OUT})}$ for any incoming polarization state S_{IN} can be obtained by

$$\begin{pmatrix} I^{(\mathrm{OUT})} \\ S_1^{(\mathrm{OUT})} \\ S_2^{(\mathrm{OUT})} \\ S_3^{(\mathrm{OUT})} \end{pmatrix} = \begin{bmatrix} M_{00} & M_{01} & M_{02} & M_{03} \\ M_{10} & M_{11} & M_{12} & M_{13} \\ M_{20} & M_{21} & M_{22} & M_{23} \\ M_{30} & M_{31} & M_{32} & M_{33} \end{bmatrix} \times \begin{pmatrix} 1 \\ \cos(2\chi)\cos(2\varphi) \\ \sin(2\chi)\cos(2\varphi) \\ \sin(2\varphi) \end{pmatrix} = M S_{\mathrm{IN}}, \qquad (4)$$

where χ and φ represent the azimuth and the ellipticity, respectively, of the incident Stokes vector on the Poincaré sphere.[15] Using Eq. (4), we can determine the Stokes vectors that produce images with both best and worst quality. This quality is defined below. Equation (4) gives all output polarization properties. Here we consider only the image intensity, $I^{(\mathrm{OUT})}$, to which only the four elements of the first row of the Mueller matrix contribute.

The parameter used to characterize image quality is the speckle noise or the inverse of the signal-to-noise ratio (often used to describe speckle[16]), defined as the ratio between the standard deviation and the mean intensity across the whole image:

$$\mathrm{SN} = (\mathrm{SNR})^{-1} = \frac{\mathrm{stdv}[I^{(\mathrm{out})}]}{\mathrm{mean}[I^{(\mathrm{out})}]}. \qquad (5)$$

In microscope mode, spatially resolved Mueller matrices were calculated for two different samples: a U.S. Air Force resolution chart and a black image on white paper (not shown here). Figure 2(a) shows the spatially resolved elements of the first row for the Mueller matrix corresponding to the U.S. Air Force target. The averaged degrees of polarization were 0.87 (nearly specular) and 0.18 (highly depolarizing) for this target and the diffuse reflection, respectively. In the ophthalmoscope mode we applied the procedure to retinal images recorded in a living human eye. In Fig. 2(b) we show the first row of the Mueller matrix for a retinal fundus region (with blood vessels).

Using these matrixes, we reconstructed images for incident light with Stokes vectors with increments of 1° for azimuth and ellipticity over the Poincaré sphere. Images were obtained for incoming polarization states that could not be generated in an experimental system. For each matrix, both the best and the worst images were reconstructed and the associated Stokes vectors calculated.

Figure 3 shows the results obtained for the specular reflection in microscope mode. The best and the worst reconstructed images as well as one of the original images are shown. Results for the retinal fundus

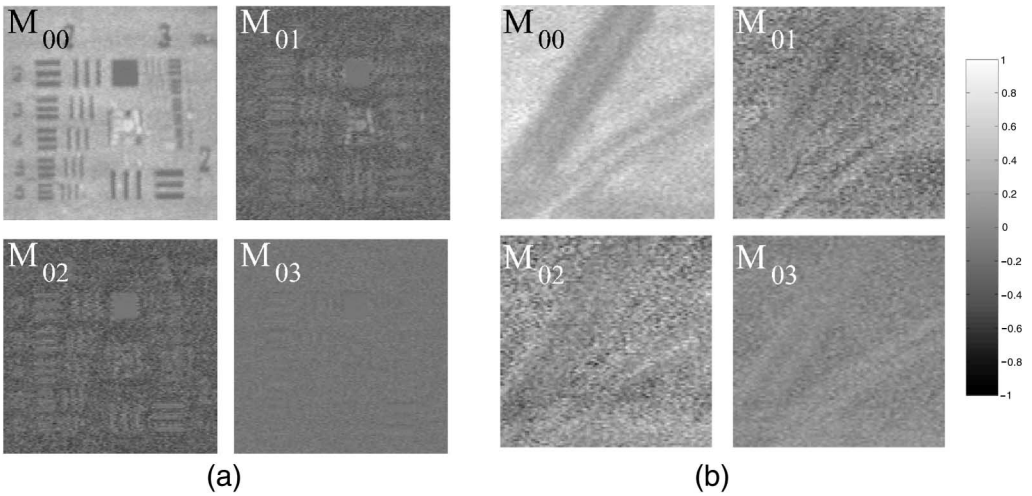

Fig. 2. Elements of the first row of the spatially resolved Mueller matrix for (a) U.S. Air Force chart (4.4 mm^2) and (b) retinal region (2°) in subject JB. The gray-level code is shown at the right.

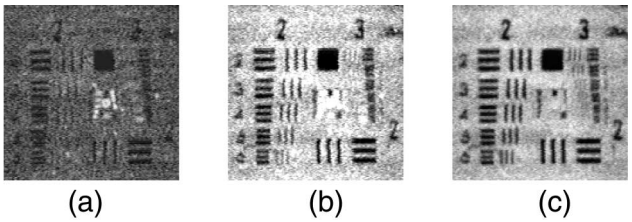

Fig. 3. Results for the target in Fig. 2: (a) worst reconstructed image, (b) original image, (c) best reconstructed image.

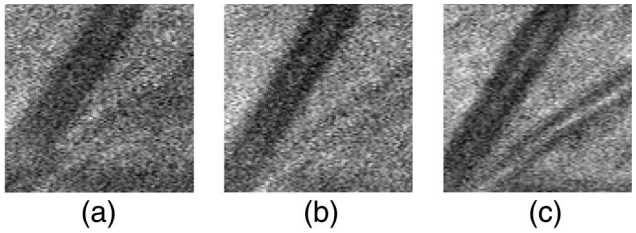

Fig. 4. (a) Worst reconstructed image, (b) original image, and (c) best reconstructed image for the fundus image in Fig. 2(b).

image are presented in Fig. 4. The original image presented is the best (lowest speckle noise or highest signal-to-noise ratio) of the images experimentally recorded. The improvement in the images obtained with this method was noticeable in all cases. Lower noise as well as higher contrast are seen in the best reconstructed image. More structural details and small features that are not discernible in the original images can also be observed. The improvement that is seen is better than that for frame averaging. Differences in the signal-to-noise ratio as defined in Eq. (5) between the original and the best images were 48% for the specular target (70% for the diffuse target) in microscope mode and 45% for the retinal fundus image. The Stokes vectors for the best specular image in Fig. 3 were $[1, -0.565, -0.099, -0.819]^T$ ($[1, 0.220, 0.604, -0.766]^T$ for the diffuse reflection), and the vectors corresponding to the optimal retinal image were $[1, 0.719, 0.262, 0.643]^T$. Moreover, an increase of as much as 30% was found in the contrast across the blood vessels of the subject presented here.

In conclusion, we have demonstrated the utility of Mueller-matrix polarimetry for improving the quality of confocal scanning microscopy and ophthalmoscopy images. The experimental system could be further improved by use of fast electro-optical modulators such as liquid-crystal variable retarders or photoelastic modulators. The polarization state that gives the best improvement in image quality differs for the specular and diffuse reflections in microscope mode and for the analyzed subject in ophthalmoscopic mode. As in imaging with polarized light,[17] the Stokes vector corresponding to the best image may vary with the characteristics of the object being measured. An implementation of this technique in commercially available ophthalmologic instruments[10,18] could enhance fundus imaging and improve diagnosis techniques.

This research was supported by the Natural Sciences and Engineering Research Council of Canada and Photonics Research Ontario. J. M. Bueno's e-mail address is bueno@um.es.

References

1. J. B. Pawley, ed., *Handbook of Biological Confocal Microscopy*, 2nd ed (Plenum, New York, 1995).
2. A. C. Ribes, S. Damaskinos, A. E. Dixon, K. A. Kellis, S. P. Duttagupta, and P. M. Fauchet, Prog. Surf. Sci. **50,** 295 (1995).
3. R. H. Webb, G. W. Hughes, and F. C. Delori, Appl. Opt. **26,** 1492 (1987).
4. J. Liang, D. R. Williams, and D. T. Miller, J. Opt. Soc. Am. A **14,** 2884 (1997).
5. I. Iglesias and P. Artal, Opt. Lett. **25,** 1804 (2000).
6. K. Muth, M. C. W. Campbell, A. J. Roorda, and C. Cui, in *Vision Science and Its Applications*, Vol. 1 of 1997 OSA Technical Digest Series (Optical Society of America, Washington, D.C., 1997), pp. 56–59.
7. M. P. Rowe, E. N. Pugh, Jr., J. S. Tyo, and N. Engheta, Opt. Lett. **20,** 608 (1995).
8. Y. Gang and L. V. Wang, Opt. Lett. **24,** 537 (1999).
9. S. Jiao, Y. Gang, and L. V. Wang, Appl. Opt. **39,** 6318 (2000).
10. A. W. Dreher, K. Reiter, and R. N. Weinred, Appl. Opt. **31,** 3730 (1992).
11. W. G. Egan, W. R. Johnson, and V. S. Whitehead, Appl. Opt. **30,** 435 (1991).
12. W. Mickols, I. Tinoco, J. E. Katz, M. F. Maestre, and C. Bustamente, Rev. Sci. Instrum. **12,** 2228 (1985).
13. R. A. Chipman, in *Handbook of Optics*, 2nd ed., M. Bass, ed. (McGraw-Hill, New York, 1995), Sect. 22.1.
14. J. M. Bueno and J. Jaronski, Opthal. Physiol. Opt. **21,** 384 (2001).
15. H. G. Jerrard, J. Opt. Soc. Am. **44,** 634 (1954).
16. J. W. Goodman, in *Laser Speckle and Related Phenomena*, 2nd ed., J. C. Dainty, ed., Vol. 9 of Topics in Applied Physics (Springer-Verlag, Berlin, 1984), pp. 9–75.
17. J. M. Bueno and P. Artal, J. Opt. Soc. Am. A **18,** 489 (2001).
18. B. Pelz, C. Weschenmoser, S. Goelz, J. P. Fischer, R. O. W. Burk, and J. F. Bille, Proc. SPIE **2930,** 92 (1996).